

A new effective interaction for $0\hbar\omega$ shell-model calculations in the $sd - pf$ valence space

F. Nowacki¹ and A. Poves²

¹*IPHC, IN2P3-CNRS et Université Louis Pasteur, F-67037 Strasbourg, France*

²*Departamento de Física Teórica e IFT-UAM/CSIC,
Universidad Autónoma de Madrid, E-28049 Madrid, Spain*

(Dated: November 8, 2018)

The neutron-rich isotopes with $Z \leq 20$, in particular those with neutron numbers around $N=28$, have been at the focus of a lot experimental and theoretical scrutiny during the last few years. Shell-model calculations using the effective interaction SDPF-NR, were able to predict or to explain most of the properties featured by these nuclei. Prominent among them is the disappearance of the $N=28$ shell closure for $Z \leq 16$. We have incorporated into SDPF-NR some modifications, either on purely theoretical grounds or guided by new experimental information. The proposed interaction SDPF-U offers enhanced reliability with respect to the earlier version.

PACS numbers: 21.10.-k, 27.40.+z, 21.60.Cs, 23.40.-s

I. INTRODUCTION

In this article we describe the reshaping of the effective interaction SDPF-NR, frequently used for $0\hbar\omega$ shell model calculations in the sd - pf valence space. This interaction originates in the work of Retamosa *et al.* [1, 2] and its final form was fixed in [3]. More details about it and some applications can be found in [4, 5], and in many of the experimental articles cited below. From the very beginning, the interest in the region was fostered by the experimental indications of a weakening (or even a complete disappearance) of the $N=28$ closure [6, 7, 8] and by the predictions of several mean-field calculations in the same sense [9, 10, 11, 12]. How can a shell closure vanish? Its persistence depends on the balance of two opposite tendencies. On the one hand, magic numbers are associated with energy gaps in the spherical mean field and this means that to promote particles above a closed shell costs energy. On the other hand, this energy can be partly recovered, because closed shells have no correlation energy, while open-shell configurations of neutrons and protons have a lot. Several examples of this phenomenon exist in stable nuclei in the form of coexisting spherical, deformed and superdeformed states in a very narrow energy range. A fully worked out case study in doubly magic ^{40}Ca can be found in [13]. At the neutron-rich edge, the structure of the spherical mean field may be at variance with the usual one at the stability line. The reason is that, at the stability line, the $T=0$ channel of the nucleon-nucleon interaction has a stronger weight relative to the $T=1$ channel than it has when the neutron excess is very large. When the gaps get reduced, open-shell configurations, usually two-neutron excitations across the neutron closure, take advantage of the availability of open-shell protons to build highly correlated states that are more bound than the closed-shell configuration. Then the shell closure is said to have vanished. ^{32}Mg is a classical reference case for this kind of physical behavior.

The interaction SDPF-NR predicts a clear breaking of

the $N=28$ magicity already at ^{44}S . The closed-shell configuration $(0f_{7/2})^8$ represents only 24% in ^{44}S , 28% in ^{42}Si , and just 3% in ^{40}Mg [5]. Its description of all the sulfur isotopes is excellent [14] and its prediction of an isomer 0^+ state just above the first 2^+ has been verified experimentally [15]. In addition, according to the calculations, the ground state of ^{43}S should be $\frac{3}{2}^-$ instead of the expected $\frac{7}{2}^-$, suggesting that this nucleus is deformed. This has been verified experimentally as well [16, 17]. Many other properties are also in agreement with the experimental data [18, 19].

The main reason that has prompted us to improve the existing effective interaction has been the vigorous renewal of interest in the region due to the access to many new neutron rich species, in particular silicon isotopes, and indeed, because of the conflicting experimental evidence on the nature of ^{42}Si coming from MSU and GANIL [15, 20, 21, 22, 23, 24, 25, 26, 27, 28]. Some of these experimental data will be analyzed in the final part of the article. As more and more experimental results are accumulated, the need for a modified version of the SDPF-NR interaction becomes more compelling.

As advanced in the title, our valence space comprises the sd shell for the valence protons, covering from $Z=8$ to $Z=20$ and the sd and pf shell for the neutrons, that is from $N=8$ to $N=40$. Notice however that below $N=20$ these calculations reduce to the pure sd -shell ones, and beyond $N=Z=20$ to pure pf -shell ones. The lightest nucleus in the valence space, that plays the role of inert core, is therefore ^{16}O . The heaviest one is ^{60}Ca . The effective interaction is composed of three blocks; sd - sd , sd - pf (proton-neutron), and pf - pf (neutron-neutron). All the shell-model calculations are unrestricted in the full sd shell for the protons and the full pf shell for the neutrons.

II. THE REFERENCE STATES

In order to improve the monopole part of the SDPF-NR interaction, we rely on the new experimental information coming from nuclei that have one particle or one hole on the top of neutron and proton closures, as well as on the values of the quasi-particle gaps across these closures. Indeed, the correlations are fully taken into account. This means that in order to find the right monopole changes several iterations are usually needed. The results for the reference states, using the new interaction SDPF-U, are compared in Table I with the experimental data (taken from the NNDC database [29] when no explicit reference is given below) and with the predictions of its precursor interaction, SDPF-NR. The neutron gap in ^{48}Ca is 4.74 MeV, compared with the experimental value, 4.78 MeV.

The nucleus ^{35}Si plays a pivotal role in fixing the evolution of the effective single-particle energies in this space. The reason is twofold; it is very single-particle-like, because of the doubly-magic character of ^{34}Si , and its neutron single-particle states define the location of the pf orbits at the neutron-rich side. That is why the changes made in the initial interaction of Retamosa *et al.* [1] to comply with the experimental finding of the low excitation energy of the $\frac{3}{2}^-$ state of ^{35}Si [3] had such important consequences in some cases. The modifications leading to the interaction SDPF-NR left the calculated centroids of the $\frac{1}{2}^-$ and $\frac{5}{2}^-$ states of ^{35}Si at their initial positions, *i.e.* similar to the ones they have in ^{41}Ca . Besides that, in order to place the $\frac{3}{2}^-$ state of ^{35}Si at its experimental excitation energy, only the $0d_{3/2}-1p_{3/2}$ centroid was modified. As a consequence, SDPF-NR produces a $\frac{1}{2}^+$ ground state in ^{49}K , instead of the $\frac{3}{2}^+$ favored by the experiments [29], and does not reproduce the assignment of $J=0^-$ to the ground state of ^{50}K proposed in [30].

Two more pieces of experimental information are considered as well; the recent study of the single-particle states in ^{47}Ar [24] that has shown a certain reduction of the spin-orbit splitting of the p orbits compared with the situation in ^{49}Ca , and the spectrum of ^{37}S [31]. Finally, the cross-shell monopoles were also constrained by requiring exact agreement with the pf -shell centroids in ^{41}Ca extracted from the $^{40}\text{Ca}(d,p)$ reaction [32].

With all these boundary conditions, the monopole part of the interaction would be uniquely defined, provided we knew the full ^{35}Si single-particle spectrum, which we do not. Among the possible choices, the one that fits most naturally with the available experimental indications [33] is that of a compressed spectrum with excitation energies 1 MeV, 2 MeV and 4 MeV for the $\frac{3}{2}^-$, $\frac{1}{2}^-$, and $\frac{5}{2}^-$ states. This time, we produce the compression by changing equally the $0d_{5/2}-r_3$, $0d_{3/2}-r_3$ and $1s_{1/2}-r_3$ centroids (r_p is a shorthand notation for all the orbits in the major oscillator shell of energy $\hbar\omega(p + \frac{3}{2})$ except the one with the largest $j = p + 1/2$). In order to obtain reasonable binding-energy differences, we have adjusted the global

TABLE I: Predictions of the SDPF-U interaction for the excitation energies of the reference states, compared with the experimental data and with the predictions of the SDPF-NR interaction (in MeV).

	J^π	EXP.	SDPF-U	SDPF-NR
^{35}Si	$\frac{7}{2}^-$	0.0	0.0	0.0
	$\frac{3}{2}^-$	0.91	0.93	0.95
	$\frac{1}{2}^-$	(2.0)	2.14	3.79
	$\frac{5}{2}^-$	—	4.16	4.76
^{35}P	$\frac{1}{2}^+$	0.0	0.0	0.0
	$\frac{3}{2}^+$	2.39	2.50	2.65
	$\frac{5}{2}^+$	3.86	3.91	4.27
^{37}S	$\frac{7}{2}^-$	0.0	0.0	0.0
	$\frac{5}{2}^-$	0.65	0.62	0.62
	$\frac{3}{2}^-$	2.51	2.44	2.44
	$\frac{1}{2}^-$	2.64	2.61	2.61
^{39}Ar	$\frac{7}{2}^-$	0.0	0.0	0.0
	$\frac{5}{2}^-$	1.27	1.54	1.37
	$\frac{3}{2}^-$	2.09	2.13	2.12
	$\frac{1}{2}^-$	—	3.08	3.02
^{41}Ca	$\frac{7}{2}^-$	0.0	0.0	0.0
	$\frac{5}{2}^-$	2.50	2.50	1.98
	$\frac{3}{2}^-$	4.16	4.20	3.97
	$\frac{1}{2}^-$	6.98	6.99	6.49
^{47}Ar	$\frac{3}{2}^-$	0.0	0.0	0.0
	$\frac{1}{2}^-$	1.13	1.14	1.28
	$\frac{5}{2}^-$	—	1.28	1.12
	$\frac{7}{2}^-$	1.74	1.58	1.37
^{47}K	$\frac{1}{2}^+$	0.0	0.0	0.0
	$\frac{3}{2}^+$	0.36	0.32	0.31
	$\frac{5}{2}^+$	3.32	3.00	2.97
^{49}K	$\frac{3}{2}^+$	(0.0)	0.0	0.074
	$\frac{1}{2}^+$	—	0.08	0.0
	$\frac{5}{2}^+$	—	0.70	0.73
^{49}Ca	$\frac{3}{2}^-$	0.0	0.0	0.0
	$\frac{1}{2}^-$	2.02	1.96	1.70
	$\frac{5}{2}^-$	3.35	3.14	2.46
	$\frac{7}{2}^-$	3.59	3.88	3.20
	$\frac{9}{2}^-$	3.99	4.03	3.83

French-Bansal monopole parameter $a = \frac{1}{4}(3\bar{V}^1 + \bar{V}^0)$ of the sd - pf interaction to the one-neutron separation energy of ^{41}Ca (8.35 MeV) and the total centroid of the neutron-neutron pf - pf interaction to the $^{52}\text{Ca} - ^{40}\text{Ca}$ mass difference. This translates into a modification of all the $T=0$ and $T=1$ sd - pf centroids of -0.045 MeV and a modification of all the $T=1$ pf - pf centroids of -0.250 MeV. If the experimental data on separation energies would demand it, extra terms quadratic in the number of sd valence protons, $n_\pi = (Z-8)$, and pf valence neutrons, $n_\nu = (N-20)$,

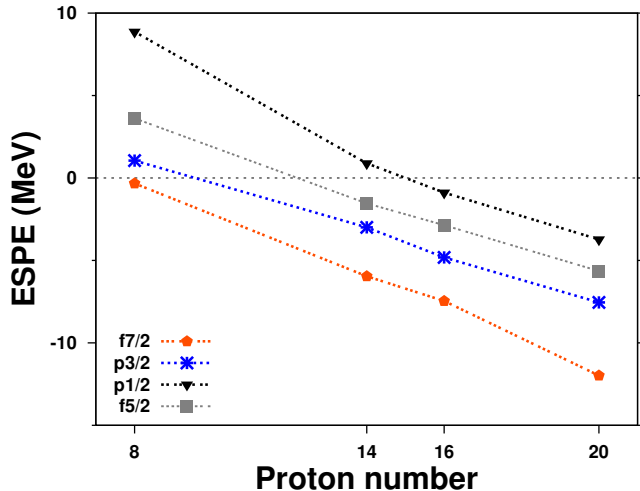


FIG. 1: (Color online) Effective neutron single-particle energies at $N=28$ from $Z=8$ to $Z=20$.

could be added to the interaction without changing its spectroscopic properties

The spherical mean field that is produced by the new interaction is better visualized by the evolution of the effective single-particle energies (ESPE) with varying proton and neutron numbers. These are presented in Figs. 1 and 2, where we plot the pf -shell neutron ESPE's at $N=28$ and $Z=8-20$, and the sd -shell proton ESPE's at $Z=20$ and $N=20-40$, respectively. In Fig. 1, we can follow the reduction of the $N=28$ neutron gap as we approach the neutron-rich edge. This reduction, combined with the degeneracy of the $0d_{3/2}$ and $1s_{1/2}$ proton orbits at $N=28$, shown in Fig. 2, is at the origin of the vanishing of the $N=28$ magicity for $Z=16$. The reason is that when the $0d_{3/2}$ and $1s_{1/2}$ are degenerate, they form a pseudo-SU3 doublet that enhances the quadrupole correlations of the configurations with open-shell neutrons. Notice also that beyond $N=28$ the orbits cross again recovering their standard ordering. The monopole part of the SDPF-U interaction (without the two global modifications discussed above) is collected in Table V at the end of the paper, and compared with the monopole part of the SDPF-NR interaction.

III. PAIRING AND THE SILICON CHAIN

The excitation energies of the first 2^+ states of the $N=22$ isotones (two neutrons in the pf -shell) are predicted too high by the SDPF-NR interaction. The deviations increase as protons are removed from ^{42}Ca till ^{36}Si . The 2^+ states of ^{38}Si and ^{40}Si are also too high by about 400 keV (this fact has been also discussed recently in [26]). However, the same interaction gives the right excitation energy for the very neutron-rich sulfur isotopes. What is the origin of this discrepancy? In our opinion, it is a subtle point of effective interaction

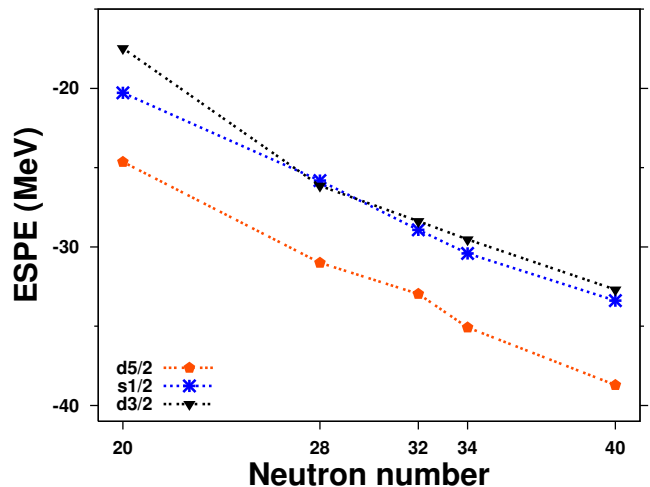


FIG. 2: (Color online) Effective proton single-particle energies in the calcium isotopes from $N=20$ to $N=40$.

theory. The pf -shell effective interaction contained in SDPF-NR is renormalized in order to compensate for the absence of $2p-2h$ excitations from the core. This renormalization, that is predominantly pairing-like, and that seems to have the right size for $Z>14$, depends on the value of the ^{40}Ca gap. However, when we deal with the silicon isotopes, the relevant gap for a perturbative estimation of the pairing renormalization is the splitting of the $0d_{5/2}$ and $0f_{7/2}$ proton orbits in ^{34}Si , which may double the former one. In addition, the off-diagonal pairing matrix element $\langle 0d_{5/2}^2(J=0) | V | 0f_{7/2}^2(J=0) \rangle$ is larger than $\langle 0d_{5/2}^2(J=0) | V | 0f_{7/2}^2(J=0) \rangle$. Using the values of the gaps and these matrix elements, we have estimated the excess of pairing renormalization for $Z \leq 14$ to be ≈ 250 keV. Therefore, we have removed from SDPF-NR a schematic pairing Hamiltonian in the pf -shell with $G = -0.09$ MeV, which, for the $\langle 0f_{7/2}^2(J=0, T=1) | V | 0f_{7/2}^2(J=0, T=1) \rangle$ matrix element represents roughly 250 keV. With this change, the 2^+ excitation energies of the silicon isotopes agree nicely with the experiment. Therefore, we have been led, and for good reasons, to have two interactions one for $Z>14$ and another for $Z \leq 14$. The files with the two versions of the SDPF-U interaction will be available with the interaction package attached to the open version of the code ANTOINE, that can be downloaded from the URL <http://sbgat194.in2p3.fr/~theory/antoine/main.html>.

IV. THE $Z=14$ GAP; DEFORMATION IN ^{42}Si

As we mentioned in the introduction, there has been recently an interesting debate on the nature of ^{42}Si , following the claim of its magic character in Ref. [20]. In a subsequent paper by the same authors [22], the claim was essentially suspended as conflicting evidence appeared. A gamma ray of very low energy observed at GANIL was

TABLE II: Properties of ^{42}Si for different effective interactions. Energies in MeV, $B(E2)$'s in $e^2 \text{ fm}^4$ and Q 's in $e \text{ fm}^2$.

	SDPF-NR	SDPF-NR ^(a)	SDPF-U
Z=14 gap	6.08	6.22	5.36
$n_\pi(0d_{5/2})$	5.42	5.43	4.83
N=28 gap	3.50	3.20	2.75
$n_\nu(0f_{7/2})$	6.16	6.55	6.08
$E^*(2^+)$	1.49	1.25	0.82
Q_s	15	16	20
BE2↓	53	48	86
Q_0 (from Q_s)	-53	-56	-70
Q_0 (from BE2)	-52	-50	-67

^(a) including the pairing correction discussed in the text.

attributed to the decay of the first excited 2^+ state. Such a low-lying 2^+ state is totally incompatible with a magic structure in this mass region [15, 27]. The interaction SDPF-NR, already indicated the vanishing of the N=28 shell closure and the development of oblate collectivity in ^{42}Si . Its predictions for ^{42}Si are gathered in the first entry of Table II. Even if the excitation energy of the 2^+ state is not low enough, the quadrupole transitions are large and consistent with the predicted (oblate) spectroscopic quadrupole moment. Besides, the occupancy, 6.16, of the $0f_{7/2}$ neutron orbit is very low, corresponding to a closed-shell percentage of 28%. This evidence was somehow masked by the too strong pf -shell pairing that we have discussed in the previous section, as can be seen clearly in the column of Table II labeled SDPF-NR^(a) (the SDPF-NR interaction including the pairing modification mentioned before). Even if the closed-shell probability increases, the quadrupole collectivity remains and the 2^+ excitation energy is now much lower. The other difference between the SDPF-NR interaction and the new SDPF-U interaction is related to the evolution of the Z=14 proton gap from N=20 to N=28. In fact, with the interaction SDPF-NR, the centroid of the (proton) $0d_{5/2}$ spectroscopic strength in ^{47}K is too high in energy compared with the experimental value extracted in [34]. The effect of reducing this gap is to lower the 2^+ excitation energy and to increase the quadrupole collectivity. Eventually, the SDPF-U interaction makes ^{42}Si a well-deformed oblate rotor with $\beta \sim 0.4$.

In Table III we have gathered the basic spectroscopic predictions of the new effective interaction for some very neutron rich silicon isotopes and compared them with the available experimental data. The quadrupole properties are computed with the effective charges $q_\nu=0.35$, $q_\nu=1.35$ that give the best reproduction of the quadrupole properties of the sd -shell nuclei [35]. The agreement with the available data is very satisfactory. The two most neutron-rich isotopes show very distinct and peculiar behaviors. In ^{42}Si , the yrast sequence 0^+ , 2^+ , 4^+ does not follow the rotational $J(J+1)$ law. However, its quadrupole properties ($B(E2)$'s and spec-

TABLE III: Basic spectroscopy of the silicon isotopes. Energies are in MeV, $B(E2)$'s in $e^2 \text{ fm}^4$ and Q 's in $e \text{ fm}^2$.

	A=36	A=38	A=40	A=42	A=44
$E^*(2_1^+)$ th.	1.36	0.96	0.80	0.82	0.87
$E^*(2_1^+)$ exp.	1.40	1.08	0.99	0.77	
BE2($2_1^+ \rightarrow 0_1^+$) th.	34	39	54	86	44
BE2($2_1^+ \rightarrow 0_1^+$) exp.	39(12)	38(14)			
$Q_s(2_1^+)$ th.	+3	-9	-9	+20	+4
$E^*(4_1^+)$ th.	2.74	1.83	1.99	1.79	2.53
S_{2n} th.	9.82	8.33	7.04	5.61	3.47

troscopic quadrupole moments) are consistent with the existence of an intrinsically-deformed oblate structure. In addition, the calculation produces a low-lying excited 0^+ state at 1.08 MeV. This state, the second-excited 2^+ state, and the second-excited 4^+ state are connected by E2 transitions of the of the same strength as those of the yrast band, but this time, the spectroscopic quadrupole moments have similar absolute values but opposite sign. This is a blatant case of coexistence of two deformed intrinsic states, one oblate and another prolate. In ^{40}Si , the $B(E2)$ values of the yrast band are smaller than the corresponding ones in ^{42}Si , while still being substantial. The calculation produces an excited 0^+ state that lies higher (1.82 MeV) and a very low-lying second-excited 2^+ state at 1.25 MeV. This 2^+ is connected by a strong E2 transition to the first 3^+ state at 1.8 MeV, forming a sort of incipient γ band.

V. THE VERY HEAVY MAGNESIUMS

The spectroscopy of the magnesium isotopes has unveiled many cases of unexpected physical behavior. The N=Z member of the chain, ^{24}Mg , is the paradigm of a well-deformed nucleus that can be described in the laboratory frame by means of Elliott's SU3 model. At N=20, ^{32}Mg is not a semi-magic nucleus but, on the contrary, a well-deformed prolate rotor. It provides one of the first examples of the vanishing of a magic closure by the action of deformed intruders [36, 37, 38]. As can be seen in table IV, the scarce experimental information on ^{34}Mg [39, 40, 41, 42] and ^{36}Mg [43] also point to well-deformed cases. We produce a ^{34}Mg less collective than the experiment, surely due to the absence of neutron excitations from the sd -shell to the pf -shell in our valence space. In ^{36}Mg , the $0\hbar\omega$ calculation already overshoots the lowering of the 2^+ state and, therefore, it does not seem necessary to resort to a large intruder mixing to explain it. When more neutrons are added, ^{38}Mg , and, prominently ^{40}Mg , are extremely deformed prolate rotors with very low 2^+ states. ^{40}Mg is at the edge of the neutron drip line, and, according to our calculations, it has nearly two neutrons in the $1p_{3/2}$ orbit, a situation that may favor the formation of a neutron halo; ^{40}Mg could then be the first well deformed nucleus adorned with a neutron halo.

TABLE IV: Basic spectroscopy of the Magnesium isotopes. Energies are in MeV, $B(E2)$'s in $e^2 \text{ fm}^4$ and Q 's in $e \text{ fm}^2$.

	A=34	A=36	A=38	A=40
$E^*(2_1^+)$ th.	0.82	0.48	0.55	0.55
$E^*(2_1^+)$ exp.	0.67	0.66		
$BE2\downarrow$ th.	65	88	101	98
$BE2\downarrow$ exp.	110(20)			
Q_s	-15	-19	-18	-20
$E^*(4_1^+)$	1.99	1.39	1.60	1.77
S_{2n} th.	7.76	6.50	4.29	2.67

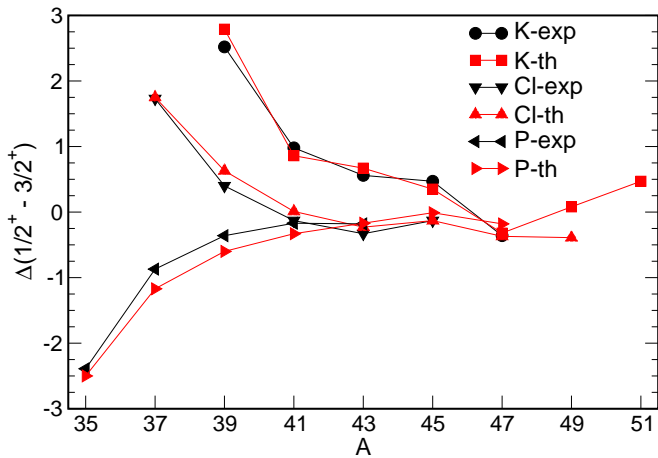


FIG. 3: (Color online) Energy splitting (in MeV) between the lowest $\frac{1}{2}^+$ and $\frac{3}{2}^+$ states in the neutron-rich isotopes of potassium, chlorine, and phosphorus.

In addition, the calculations suggest that in ^{40}Mg , the prolate yrast band may coexist with an oblate one based in an excited 0^+ state at 2.07 MeV, in parallel with the situation found in ^{42}Si . ^{38}Mg is, according to our description, a triaxial rotor in view of the presence of a γ band based upon the second 2^+ state at 1.07 MeV excitation energy. This band comprises the first 3^+ and the second 4^+ states. The energies and the ratios of the transitions between the two bands are consistent with $\gamma=0.2$. Similar triaxial structures have been recently shown in the heaviest Argon isotopes [44].

VI. THE EVOLUTION OF THE $\frac{1}{2}^+ - \frac{3}{2}^+$ SPLITTING IN THE K, CL AND P ISOTOPES

In Fig. 3, we present the evolution of the energy splitting between the lowest $\frac{1}{2}^+$ and $\frac{3}{2}^+$ states in the neutron-rich isotopes of potassium, chlorine and phosphorus. Notice in the first place the excellent agreement of the theoretical predictions with the available experimental data. In the limit of pure single-particle behavior, the points should lie on straight lines joining the neutron closures $N=20$, $N=28$ and $N=32$, corresponding to the ones in

Fig. 2 for the potassium chain. This is clearly not the case, because of the coupling of the proton-single particle states with the neutron excitations. As we can gather from the figure, the splitting in the potassiums drops rapidly when two neutrons are added to the $N=20$ closure, meaning that the states have not a single-particle character anymore. At $N=28$ the single-particle behavior is recovered and the inversion of the two states that takes place is dictated by the effective single-particle energies. The crossing of the two orbits just reflects the fact that the neutron-proton interaction is more attractive between the orbits $0f_{7/2}$ and $0d_{3/2}$ than between the orbits $0f_{7/2}$ and $1s_{1/2}$. When neutrons fill the $1p_{3/2}$ orbit, the opposite is true and the ground-state spins of ^{49}K and ^{51}K bounce back to $\frac{3}{2}^+$. The situation is less clear cut in the chlorines, because its three proton holes produce enhanced mixing. This can be seen also in Fig. 3; at $N=20$, ^{37}Cl has the normal ordering of spins that corresponds to a ground-state proton configuration $(1s_{1/2})^2 (0d_{3/2})^1 J = \frac{3}{2}^+$ with an excited $\frac{1}{2}^+$ state corresponding to the configuration $(1s_{1/2})^1 (0d_{3/2})^2$. Increasing the number of neutrons reduces the $0d_{3/2} - 1s_{1/2}$ splitting and increases the mixing among different proton configurations. Already at $N=26$ both states approach the configuration $(1s_{1/2})^1 (0d_{3/2})^2$ and become nearly degenerate as the protons enter in a pseudo-SU3 regime. The heavy chlorines may be viewed as one proton coupled to the corresponding $(A-1)$ sulfur isotope. At $N=26$, ^{42}S is deformed and at $N=28$ the neutron closure has vanished in ^{44}S ; this explains why, in the chlorine chain, there is no trace of the single-particle effects that are so visible in the potassium chain when we cross $N=28$. *Mutatis mutandis*, these arguments hold for the phosphorus isotopes.

VII. CONCLUSIONS

In summary, we have produced a new effective interaction, SDPF-U, suitable for unrestricted $0\hbar\omega$ large-scale shell-model calculations in the $sd - pf$ valence space, for nuclei with proton number ranging from $Z=8$ to $Z=20$ and neutron number from $N=20$ to $N=40$. We have presented a first series of theoretical predictions and have compared them with the experimental results. Special attention has been devoted to the behavior of the neutron rich silicon and magnesium isotopes and to the vanishing of the $N=28$ neutron shell closure in ^{42}Si and ^{40}Mg . We have also explored the evolution of the energy splitting between the lowest $\frac{1}{2}^+$ and $\frac{3}{2}^+$ states in the neutron-rich isotopes of potassium, chlorine and phosphorus, finding an excellent agreement with the experimental results.

Acknowledgments. The authors express their warmest thanks to Etienne Caurier for his help in different aspects of this work. Partly supported by a grant of the Spanish Ministry of Education and Science (FPA2007-66069), by the IN2P3(France)-CICyT(Spain)

TABLE V: Centroids of the SDPF-U(*) and SDPF-NR interactions for A=18 (in MeV). The standard mass dependence $(A/18)^{1/3}$ is adopted in the calculations. The single particle energies (in MeV) on a core of ^{16}O are the following: $0d_{5/2}=-3.70$; $1s_{1/2}=-2.92$; $0d_{3/2}=1.90$; $0f_{7/2}=6.22$; $1p_{3/2}=6.31$; $0f_{5/2}=11.45$; $1p_{1/2}=6.48$.

j_1	j_2	T	SDPF-U	SDPF-NR
$0d_{5/2}$	$0d_{5/2}$	0	-3.19	-3.19
$0d_{5/2}$	$0d_{5/2}$	1	-0.53	-0.61
$0d_{5/2}$	$1s_{1/2}$	0	-3.12	-3.12
$0d_{5/2}$	$1s_{1/2}$	1	0.14	0.14
$0d_{5/2}$	$0d_{3/2}$	0	-3.74	-3.74
$0d_{5/2}$	$0d_{3/2}$	1	-0.33	-0.29
$1s_{1/2}$	$1s_{1/2}$	0	-3.51	-3.51
$1s_{1/2}$	$1s_{1/2}$	1	-2.15	-2.15
$1s_{1/2}$	$0d_{3/2}$	0	-3.01	-3.01
$1s_{1/2}$	$0d_{3/2}$	1	0.00	0.00
$0d_{3/2}$	$0d_{3/2}$	0	-2.67	-2.67
$0d_{3/2}$	$0d_{3/2}$	1	-0.31	-0.40
$0d_{5/2}$	$0f_{7/2}$	0	-2.55	-2.85
$0d_{5/2}$	$0f_{7/2}$	1	0.00	0.00
$0d_{5/2}$	$1p_{3/2}$	0	-1.51	-2.50
$0d_{5/2}$	$1p_{3/2}$	1	-0.31	-0.08
$0d_{5/2}$	$0f_{5/2}$	0	-3.17	-4.16
$0d_{5/2}$	$0f_{5/2}$	1	-0.32	-0.09
$0d_{5/2}$	$1p_{1/2}$	0	-1.77	-3.25
$0d_{5/2}$	$1p_{1/2}$	1	-0.48	-0.08
$1s_{1/2}$	$0f_{7/2}$	0	-1.89	-1.89
$1s_{1/2}$	$0f_{7/2}$	1	-0.30	-0.30
$1s_{1/2}$	$1p_{3/2}$	0	-1.44	-1.07
$1s_{1/2}$	$1p_{3/2}$	1	-1.12	-1.41
$1s_{1/2}$	$0f_{5/2}$	0	-2.48	-3.17
$1s_{1/2}$	$0f_{5/2}$	1	-0.05	0.18
$1s_{1/2}$	$1p_{1/2}$	0	-1.91	-4.21
$1s_{1/2}$	$1p_{1/2}$	1	0.05	0.43
$0d_{3/2}$	$0f_{7/2}$	0	-2.43	-2.43
$0d_{3/2}$	$0f_{7/2}$	1	-0.88	-0.88
$0d_{3/2}$	$1p_{3/2}$	0	-1.72	-2.26
$0d_{3/2}$	$1p_{3/2}$	1	-0.30	-0.15
$0d_{3/2}$	$0f_{5/2}$	0	-2.39	-3.08
$0d_{3/2}$	$0f_{5/2}$	1	0.27	0.50
$0d_{3/2}$	$1p_{1/2}$	0	-2.05	-2.79
$0d_{3/2}$	$1p_{1/2}$	1	0.03	0.41
$0f_{7/2}$	$0f_{7/2}$	1	-0.27	-0.37
$0f_{7/2}$	$1p_{3/2}$	1	0.15	0.12
$0f_{7/2}$	$0f_{5/2}$	1	0.03	-0.04
$0f_{7/2}$	$1p_{1/2}$	1	0.20	0.07
$1p_{3/2}$	$1p_{3/2}$	1	-0.10	-0.81
$1p_{3/2}$	$0f_{5/2}$	1	0.36	-0.16
$1p_{3/2}$	$1p_{1/2}$	1	0.16	-0.62
$0f_{5/2}$	$0f_{5/2}$	1	0.12	-0.07
$0f_{5/2}$	$1p_{1/2}$	1	0.14	-0.05
$1p_{1/2}$	$1p_{1/2}$	1	0.25	-0.46

(*) without the global monopole corrections (see text).

collaboration agreements, by the Spanish Consolider-Ingenio 2010 Program CPAN (CSD2007-00042) and by the Comunidad de Madrid (Spain), project HEPHACOS P-ESP-00346.

[1] J. Retamosa, E. Caurier, F. Nowacki, and A. Poves, Phys. Rev. C **55**, 1266 (1997).

[2] E. Caurier, F. Nowacki, A. Poves, and J. Retamosa, Phys. Rev. C **58**, 2033 (1998).

- [3] S. Nummela *et al.*, Phys. Rev. C **63**, 044316 (2001).
- [4] E. Caurier, G. Martínez-Pinedo, F. Nowacki, A. Poves, and A. P. Zuker, Rev. Mod. Phys. **77**, 427 (2005).
- [5] E. Caurier, F. Nowacki, and A. Poves, Nucl. Phys. **A742**, 14 (2004).
- [6] O. Sorlin *et al.*, Phys. Rev. C **47**, 2941 (1993).
- [7] O. Sorlin *et al.*, Nucl. Phys. **A583**, 763 (1995).
- [8] S. Grévy *et al.*, Phys. Lett. **B594**, 252 (2004).
- [9] P. G. Reinhard, D. J. Dean, W. Nazarewicz, J. Dobaczewski, J. A. Maruhn, and M. R. Strayer, Phys. Rev. C **60**, 014316 (1999).
- [10] G. A. Lalazissis, D. Vretenar, P. Ring, M. Stoitsov, and L. Robledo, Phys. Rev. C **60**, 014310 (1999).
- [11] S. Peru *et al.*, Eur. Phys. J. A **9**, 35 (2000).
- [12] R. Rodríguez-Guzmán, J. L. Egido, and L. M. Robledo, Phys. Rev. C **65**, 024304 (2002).
- [13] E. Caurier, J. Menéndez, F. Nowacki, and A. Poves, Phys. Rev. C **75**, 054317 (2007).
- [14] D. Sohler *et al.*, Phys. Rev. C **66**, 054302 (2002).
- [15] S. Grevy *et al.*, Eur. Phys. J. A **25**, 111 (2005).
- [16] F. Sarazin *et al.*, Phys. Rev. Lett. **84**, 5062 (2000).
- [17] R. W. Ibbotson, T. Glasmacher, P. F. Mantica, and H. Scheit, Phys. Rev. C **59**, 642 (1999).
- [18] Zs. Dombrádi *et al.*, Nucl. Phys. **A727**, 195 (2003).
- [19] A. E. Stuchbery *et al.*, Phys. Rev. C **74**, 054307 (2006).
- [20] J. Fridmann *et al.*, Nature **435**, 922 (2005).
- [21] A. Gade *et al.*, Phys. Rev. C **71**, 051301(R) (2005).
- [22] J. Fridmann *et al.*, Phys. Rev. C **74**, 034313 (2006).
- [23] B. Jurado *et al.*, Phys. Lett. **B649**, 43 (2007).
- [24] L. Gaudefrey *et al.*, Phys. Rev. Lett. **97**, 092501 (2006).
- [25] A. Gade *et al.*, Phys. Rev. C **74**, 034322 (2006).
- [26] C. M. Campbell *et al.*, Phys. Rev. Lett. **97**, 112501 (2006).
- [27] B. Bastin *et al.*, Phys. Rev. Lett. **99**, 022503 (2007).
- [28] C. M. Campbell *et al.*, Phys. Lett. **B652**, 169 (2007).
- [29] National Nuclear Data Center, Brookhaven National Lab. 2008. <http://www.nndc.bnl.gov>.
- [30] P. Baumann *et al.*, Phys. Rev. C **58**, 1970 (1998).
- [31] P. M. Endt and R. B. Firestone, Nucl. Phys. **A633**, 1 (1988).
- [32] Y. Uozumi *et al.*, Phys. Rev. C **50**, 263 (1994).
- [33] M. Gelin *et al.*, in *Proceedings of the INPC2007 Conference* (Tokyo), edited by S. Nagamiya, T. Motobayashi, M. Oka, R. S. Hayano and T. Nagae (Elsevier, Amsterdam, 2008), Vol. II, p.368.
- [34] G. J. Kramer *et al.*, Nucl. Phys. **A679**, 267 (2001).
- [35] B. A. Brown and B. H. Wildenthal, Ann. Rev. Nucl. Part. Sci. **38**, 29 (1988).
- [36] D. Guillemaud-Mueller *et al.*, Nucl. Phys. **A426**, 37 (1984).
- [37] T. Motobayashi *et al.*, Phys. Lett. **B346**, 9 (1995).
- [38] A. Poves and J. Retamosa, Phys. Lett. **B184**, 311 (1987).
- [39] K. Yoneda *et al.*, Phys. Lett. **B499**, 233 (2001).
- [40] H. Iwasaki *et al.*, Phys. Lett. **B522**, 227 (2001).
- [41] J. A. Church *et al.*, Phys. Rev. C **72**, 054320 (2005).
- [42] Z. Elekes *et al.*, Phys. Rev. C **73**, 044314 (2006).
- [43] A. Gade *et al.*, Phys. Rev. Lett. **99**, 072502 (2007).
- [44] S. Bhattacharyya *et al.*, Phys. Rev. Lett. **101**, 032501 (2008).